American Journal of
Nanoscience and Nanotechnology Research
http://www.ivyunion.org/index.php/ajnnr

Research Article

Characterization of Green Synthesized Silver Nanoparticles Doped in Polyacrylonitrile Nanofibers

Moeng G. Motitswe[1,2], Omolola E. Fayemi[1,2*]

[1] Department of Chemistry, Faculty of Natural and Agricultural Sciences, North-West University (Mafikeng Campus), South Africa

[2] Material Science Innovation and Modelling (MaSIM) Research Focus Area, Faculty of Natural and Agricultural Sciences, North-West University (Mafikeng Campus), South Africa

Abstract: This paper reports a cost effective and eco-friendly green technique used for the synthesis of silver metal nanoparticle from orange peel extracts. The synthesized nanoparticle was functionalized with polyacrylonitrile to form PAN/Ag nanofibers by electrospinning. The synthesized nanoparticle and its nanofibers were characterized by using spectroscopic and morphology techniques such as fourier transform infrared (FT-IR) spectroscopy, ultraviolet-visible (UV-vis) spectroscopy, x-ray diffraction (XRD) spectroscopy, scanning electron microscopy (SEM), EDX to determine the elemental composition of the nanofibers and transmission electron microscope (TEM). The optical studies for the silver nanoparticles were carried out at different concentrations, volumes, and incubation time. The nanofiber diameters were evaluated to be 11, 9, 8, 6 nm for PAN , 6 mg Ag + PAN, 8 mg Ag+ PAN, and 10 mg Ag + PAN nanofibers. SEM of silver nanoparticles showed uniformity in morphology of which is spherical shape, with diameter of 20 nm. Thermal stability of the nanofibers was also investigated using thermal gravimetric analysis.

Keywords: Green Synthesis, Silver nanoparticle, Polyacrylonitrile, Electrospinning, Uv-Vis spectroscopy

Received: November 6, 2018; **Accepted**: December 21, 2018; P**ublished**: January 29, 2019

Competing Interests: The author has declared that no competing interests exist.

***Correspondence to**: Material Science Innovation and Modelling (MaSIM) Research Focus Area, Faculty of Natural and Agricultural Sciences, North-West University (Mafikeng Campus), South Africa

Email: Omolola.Fayemi@nwu.ac.za

1. Introduction

The introduction of green synthesis into nanotechnology has gained intense attraction due to the range of chemical and physical properties of nanomaterials at nano level. Different methods have been employed for the synthesis of nanoparticles such as laser ablation, microwave, wet chemical methods, micro emulsion and gamma irradiation. Green methods with the use of plant materials (as reducing agents) are gradually adopted because of their eco-friendliness and cost effective. A range of metal nanospecies have been synthesized by these methods. Amongst the green synthesized nanostrustures are copper nanoparticles which have been fabricated by reductive capability of Moringa morindoides plant [1]. It was evidently shown that nanofabrication of palladium, platinum, and gold metal nanoparticles has been achieved by use of Cinnamon zeylanicum (cinnamon), Azadirachta indica, and Trigonella-foenum graecum as reducing and stabilization agent [2-4].

Reports showed that the other biological way for silver nanometal synthesis was established through marine algae Caulerpa racemosa and Bacillus strain CS 11 [5-6]. Further utilization of the green method has been performed for bioreduction of gold and silver ions by various plants such as Pelargonium graveolens, Tamarindus indica (tamarind) leaf extract and Azadirachta indica [7-8]. Additionally, the biosynthesis of silver nanoparticles has been established with Ocimum sanctum leaf extract and Musa paradisiaca (banana peel extracts) [9-10]. Silver nanoparticles have properties such as unique antimicrobial and antiviral activity, electrical and optical feature, stability, large surface area and size (< 100 nm). Consequently, their applications are felt in clinics (medicines), energy production sectors (solar cells, supercapacitors) [11], drug delivery services [12], and sensors. The most remarkable silver nanoparticles' application is their ability to be used in treatment of diseases, such as HIV-1 virus and counter acting its power to bind host cells [13]. Silver nanoparticle based nanocomposites have been nano-implemented for various applications in nutrition, pharmaceutical, and nanoelectronics. Research program showed that these nanoparticles were embedded into hydroxypropyl methylcellulose for food packaging components [14], silver nanoparticles-graphene-polypyrrole for phenomenal supercapacitor [15], silver nanoparticle-polysulfone membranes for enhanced antibacterial activity [16]. Functionalization of chitosan/poly (vinyl alcohol) blend with silver nanoparticles for prostate cancer tumour treatment has been reported [17]. Silver nanoparticle-polyaniline nanofibers have been used for electrochemical sensing of H_2O_2, glucose and ethanol vapour [18-19].

Polymer nanofibers are fabricated by use of self-assembly, melt compounding, electrochemical, in situ polymerization and template based synthesis. However, wide range of nanofibers have been produced by using the method electrospinning because of its capability to produce tunable and uniform diameters, long fiber, ease of operation, eco-friendliness, and miniaturized property. Different polymers have been used for the formation of nanofibers. Example of some of the polymeric molecules are poly-p-phenylenes (PPVs), polyaniline (PANI), poly (lactic acid) (PLA), polypyrrole (PPy), and polyethylene oxide (PEO) [20-23]. Polyacrylonitrile has properties such as high melting point (~317 ℃), and its fibers' distinctive mechanical property (due to intermolecular forces in the chain and electrostatic forces occurring in between dipoles of –C=N). Its mechanical property also tends to limit the extent of degradation of the molecule and being advantageous for further reaction processes and applications. Polyacrylonitrile nanofibers possess upgraded sensitivity and faster response time scale due to high surface area and shorter penetration distance for target species. Therefore, these characteristics are of importance in various applications such as water specimen sensing and nanofiltration.

Nanocomposites have been used for various vast functionalities and applications. In particular, polyacrylonitrile (PAN) nanocomposites have been fabricated in various methods. CdS/polyacrylonitrile, Ag/polyacrylonitrile, and PbS/polyacrylonitrile nanocomposites have been synthesized by gamma irradiation [24-26]. Research study showed that Ni/C based polyacrylonitrile nanocomposites were synthesized by IR-radiation [27]. Additionally, Na−MMT/polyacrylonitrile nanocomposites underwent synthesis by emulsion polymerization of the monomer [28]. Titanium dioxide and silver nanoparticles were used to functionalize the polyacrylonitrile surface by wet spinning method for generation of filaments with good electrical, and photocatalytic properties [29]. Iron nanoparticles have been used for construction of polyacrylonitrile nanocomposites through liquid-liquid extraction method [30]. Furthermore, polyacrylonitrile reinforced with silver nanoparticles were electrospun for bacterial based membrane filtration [31]. Synthesized nanocomposite of SWCN/polyacrylonitrile has led to high performing membranes for decrementation of wastewater' biological and chemical contamination indicators [32]. Pronounced functionalized polyacrylonitrile nanocomposites with zinc oxide and tin (IV) oxide nanoparticles exhibited improved light photocatalytic activity [33-34]. TiO_2/polyacrylonitrile nanofiber composite were applied for adsorptive capability towards lead ions from the waste water [35]. Ag/amino-terminated hyperbranched polymer (HBP)/polyacrylonitrile (PAN) nanocomposites showed optimal antimicrobial and filtrating capability on microbial product such E. coli and S. aureus [36]. Silver nanoparticles possessed adsorptive and inhibitive layer in polyacrylonitrile nanofiber incorporated within the fabrics of human nose masks for antibacterial avtivity [37]. In nanoelectronics, polyacrylonitrile has been used for yielding porous silicon particulates for application in lithium ion [38]. Ag/polacrylonitrile composite extended its prominent effect in formation of unique membrane for reliable and simple water filtration [39-40]. Research studies show that Ag/polacrylonitrile nanocomposite's good permeability is well applied towards various specimens especially in water, catalysis, and safety garments [41-43].

Therefore this study reports the green mediated synthesis of silver nanoparticles and characterization of silver nanoparticles doped in polyacrylonitrile nanofibers containing different concentration of silver nanoparticles which is scarce in literature. The materials were characterized with Uv-Vis, FTIR, SEM, TEM, ZetaSizer, and TGA.

2. Experimental Part

2.1 Chemicals

Polyacrylonitrile (Mw = 150 000), silver nitrate were purchased from Sigma-Aldrich Co. These chemicals were analytical grade and were used as received.

2.2 Preparation of Silver Nanoparticles from Orange Peel Extracts

Peeled sweet ripe oranges (Citrus Sinensis) were washed with distilled water, sun dried for two consecutive days and were crushed into finer particles. About 2 g of peel powder were boiled in 70 ml of distilled water, filtered and stored at 7 ^{o}C for further use. Consequently, about 50 ml of aqueous solution (0.2 M) of $AgNO_3$ was mixed with the extract solution (40 ml) and allowed to stir for about 28 h at room temperature. An enhanced yield of deep reddish amber colour of AgNPs was produced.

2.4 Nanofabrication of PAN nanofibers and PAN/Ag nanocomposites

PAN powder (1.65 g) was pre-dried at 60 ℃ for 24 h and then dissolved in 15 ml of DMF. The mixture was magnetically stirred under room temperature overnight. Thereafter, electrospinning apparatus

were configured by filling the 20 ml syringe with the prepared PAN solution (11 % wt.). The spinning parameters were set as follow: applied potential (22 kV), spinning distance (13 cm), and flow rate (0.050 ml/min). Aluminium foil plate was used as a ground collector and spinning was carried out at room temperature. The removal of DMF from the nanofibers was performed by drying the electrospun nanofibers under room temperature overnight in the fume hood line. From the prepared PAN solution, 7.5 ml of it was mixed with different concentration of silver nanoparticles [4, 6, 8, 10 mg] and the binary mixture was stirred overnight for complete dissolution. Afterwards, the above mentioned spinning parameters were sustained during electrospinning process. The composite nanofibers formed were dried at 25 ºC overnight in the fume hood, respectively.

2.5 Characterization of synthesized AgNPs and PAN/Ag nanofibers.

Silver nanoparticles and silver doped in polyacryonitrile were characterized by using FT-IR spectrometer joined to a PerkinElmer Auto image microscope system equipped with liquid nitrogen cooled MCT detector, morphological images were obtained by utilising scanning electron microscopy bought from Japan (JEOL JSM 5800 LV), and the elemental composition of the nanoparticle and the nanofibers were also investigated. The Zeta potential for the nanoparticle was obtained by using Zeta Analyzer.

3. Results and discussion

3.1 Characterization of synthesized nanomaterials

3.1.1 UV-Visible characterization of AgNPs

Absorption spectrum of silver nanoparticles synthesized from $AgNO_3$ treated with orange peel extracts exhibited characteristic peaks at wavelength (425- 450 nm) as shown in Figure 1 (a - d). According to literature, nanofabrication of silver nanoparticles can be achieved at characteristic surface plasmon absorption peaks ranging from 420 to 470 nm [44]. Figure 1 (b) revealed that as the time retrieval of aliquots increases, the absorbance intensity of the nanoparticle increases. It further confirms that absorbance is time dependent during the synthesis, therefore the highest absorbance was achieved at 28 h and the lowest at 1 h. Figure 1 (c) shows the effect of precursor concentration on the characteristics peak absorbance of the nanoparticle formed. The higher the concentration of the precursor, the greater the absorbance. Also, an increase in extract concentrations showed positive growth in relation with absorbance of the synthesized nanoparticles as shown in Figure 1 (d**)**. Successful synthesis of AgNPs was confirmed by the deep reddish amber colour [45]. This physical property has been used to confirm the synthesis [46] in conjunction with UV–vis spectroscopy technique [47-48]. The characteristic colour differences and absorbance are due to surface resonance which is caused by nanoparticles' oscillatory movement of electron in resonance with the light radiation [49-50].

The band energy, E (eV) was calculated from the Uv-visible absorption spectra by using the following Einstein's photon energy equation 1 and the results of parameters determined are represented in Tables 1 to 3. An optimisation studies was carried out during the synthesis of the silver nanoparticles by varying the incubation time, concentration of precursor and the volume of the extract.

$$E = \frac{hc}{\lambda} \quad (1)$$

The results generally reveals that as the incubation time, concentration of precursor and the volume of extracts increases there was a shift in wavelength which is evidence by the increase in absorption band.

Consequently, there was also a decrease in the conduction band energy which resulted to a decrease in band gap. Optical band energy for synthesized silver nanoparticles under various time intervals was evaluated as 2.1 eV. Therefore, conduction band energy of Ag nanoparticles is in closer relativity to the documented values, 2.7 and 2.5 eV [51-52].

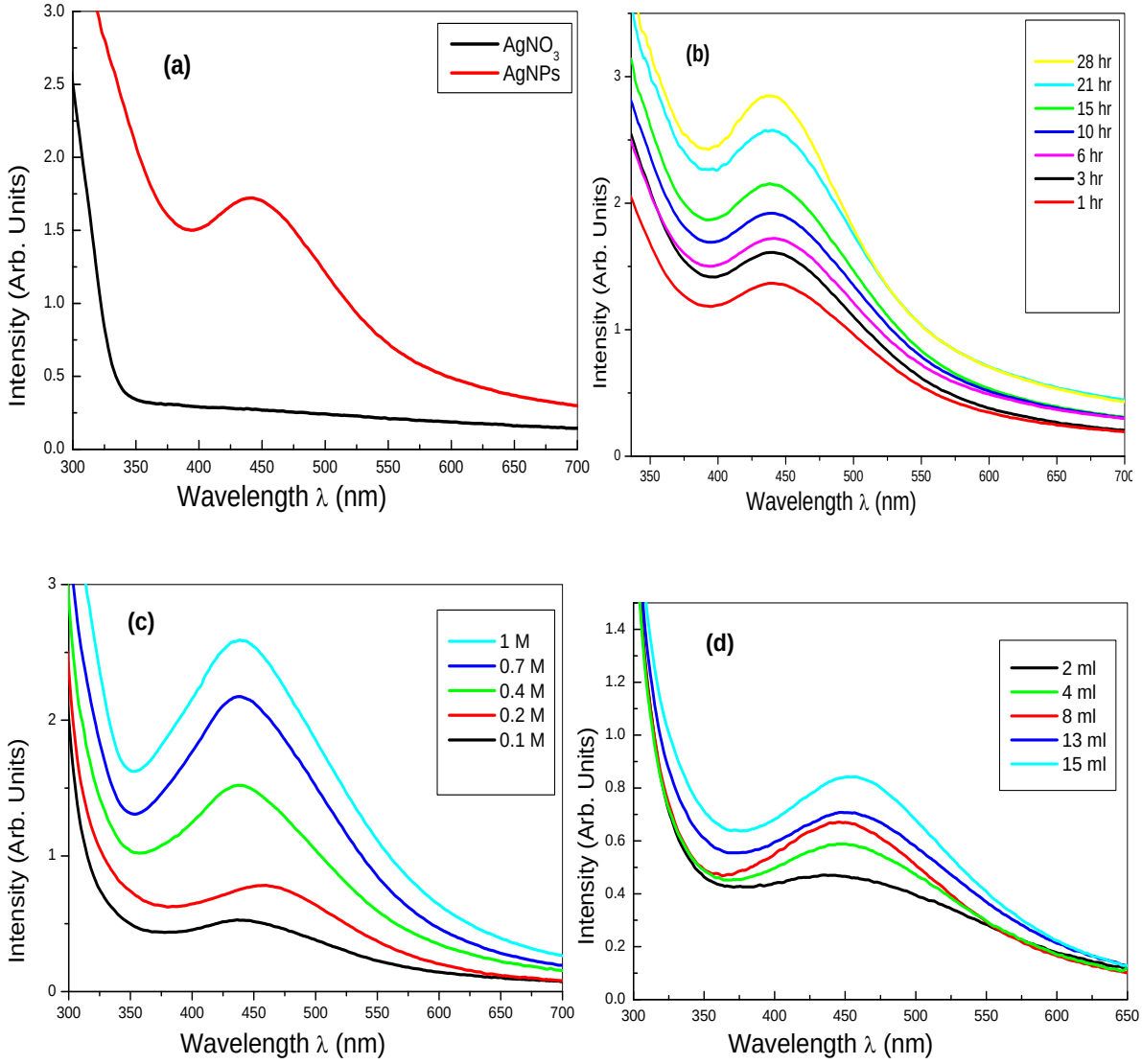

Fig. 1 UV-vis spectra of (a) precursor and AgNPs and synthesized AgNPs nanoparticles at (b) incubation time of 1 – 28 h (c) different precursor concentrations, (d) different extract volumes

Table 1 Band gap of synthesized Ag nanoparticles at different incubation times

Time (hours)	h	c	λ	E	eV
1	6.63×10^{-34}	3×10^{8}	574×10^{-9}	3.4651567×10^{-19}	2.165723
3	6.63×10^{-34}	3×10^{8}	582×10^{-9}	3.4175258×10^{-19}	2.1359536
6	6.63×10^{-34}	3×10^{8}	587×10^{-9}	3.3884157×10^{-19}	2.1177597
10	6.63×10^{-34}	3×10^{8}	590×10^{-9}	3.3711864×10^{-19}	2.1069915
15	6.63×10^{-34}	3×10^{8}	596×10^{-9}	3.3372483×10^{-19}	2.0857802
21	6.63×10^{-34}	3×10^{8}	601×10^{-9}	3.3094842×10^{-19}	2.0684276
28	6.63×10^{-34}	3×10^{8}	606×10^{-9}	3.2821782×10^{-19}	2.0513614

Table 2 Band gap of synthesized Ag nanoparticles at different concentrations of the precursor ($AgNO_3$)

Concentration (M)	h	c	λ	E	eV
0.1	6.63×10^{-34}	3×10^{8}	541×10^{-9}	3.6765249×10^{-19}	2.2978281
0.2	6.63×10^{-34}	3×10^{8}	560×10^{-9}	3.5517857×10^{-19}	2.2198661
0.4	6.63×10^{-34}	3×10^{8}	573×10^{-9}	3.4712042×10^{-19}	2.1695026
0.7	6.63×10^{-34}	3×10^{8}	585×10^{-9}	3.4000000×10^{-19}	2.1250000
1	6.63×10^{-34}	3×10^{8}	607×10^{-9}	3.2767710×10^{-19}	2.0479818

Table 3 Band gap of synthesized Ag nanoparticles at different volume of the extracts

Extracts Volume (ml)	h	c	λ	E	eV
2	6.63×10^{-34}	3×10^{8}	538×10^{-9}	3.697026×10^{-19}	2.3106413
4	6.63×10^{-34}	3×10^{8}	540×10^{-9}	3.683333×10^{-19}	2.3020831
8	6.63×10^{-34}	3×10^{8}	544×10^{-9}	3.656250×10^{-37}	2.2851563
13	6.63×10^{-34}	3×10^{8}	553×10^{-9}	3.596745×10^{-37}	2.2479656
15	6.63×10^{-34}	3×10^{8}	570×10^{-9}	3.489474×10^{-37}	2.1809211

3.1.2 UV-visible characterization of PAN and PAN/Ag nanofibers

The optimised silver nanoparticle was then doped with polyacryonitrile nanofibers. The UV-vis spectra of the nanofibers of PAN and PAN/Ag at different concentration of AgNPs are shown in Figure 2. The achieved characteristic wavelength for polyacrylonitrile nanofibers was at 350 nm .The incorporated silver nanoparticles displayed characteristic peak at 420 nm, with varying absorbance due to silver nanoparticles mass contents, respectively. Embedment of these nanoparticles in the nanofibers enhances the electrical conductivity of the nanocomposites [53].

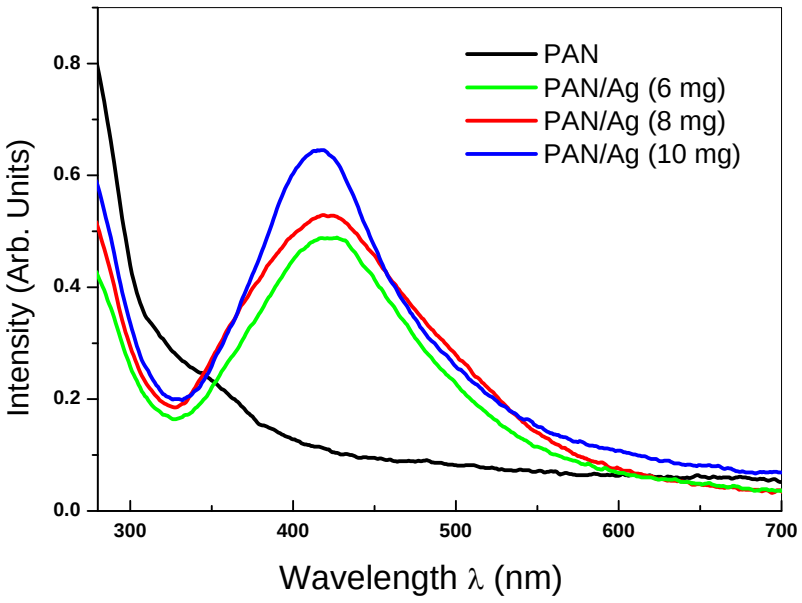

Fig. 2 Uv-vis spectrum of electrospun PAN (11 % w.) and composites of various silver nanoparticle concentrations.

3.1.3 FTIR characterization of AgNPs

FTIR measurements shown in Figure 3 were carried out by scanning in the range 500–4000 cm^{-1}**.** The characteristic peaks at 3291, and 2922 cm^{-1} represent the presence of alcohol/phenol O-H, and alkyl C-H stretches, respectively. Stretch at 2349 cm^{-1} is attributed to O=C=O, which can be attributed to organic carbon from extracts chelating with oxygen of nitrate group. Band seen at 2107 cm^{-1} was assigned to alkynyl C≡C stretch, respectively. Ketone/Carboxylic acid C=O stretch is seen at 1739 cm^{-1}. The intense band (in extracts) seen at 1603 cm^{-1} can be conveyed to N–H amine group in peels and can serve as an evidence of reducing constituent on the nanoparticles. Pronounced vibrational mode seen at 1292 cm^{-1} in nanoparticles may be caused by C-N stretching mode (N from silver nitrate), thus indication that the orange peel extract was responsible for reduction of silver nanoparticles ($Ag^{+} \rightarrow Ag^{0}$). On formation of silver nanoparticles, the peak corresponding to the silver band at 794 cm^{-1} (in the precursor) as compared to the one at 786 cm^{-1} (in the nanoparticles) has broadened a bit and shortened, this implied capping of the silver nanoparticles by flavonoids. The band observed at 1020 cm^{-1} can be

assigned to the C–N stretching vibration of aliphatic amine. This observation indicates the presence and binding of orange extracts with silver nanoparticles which can result to their possible stabilization.

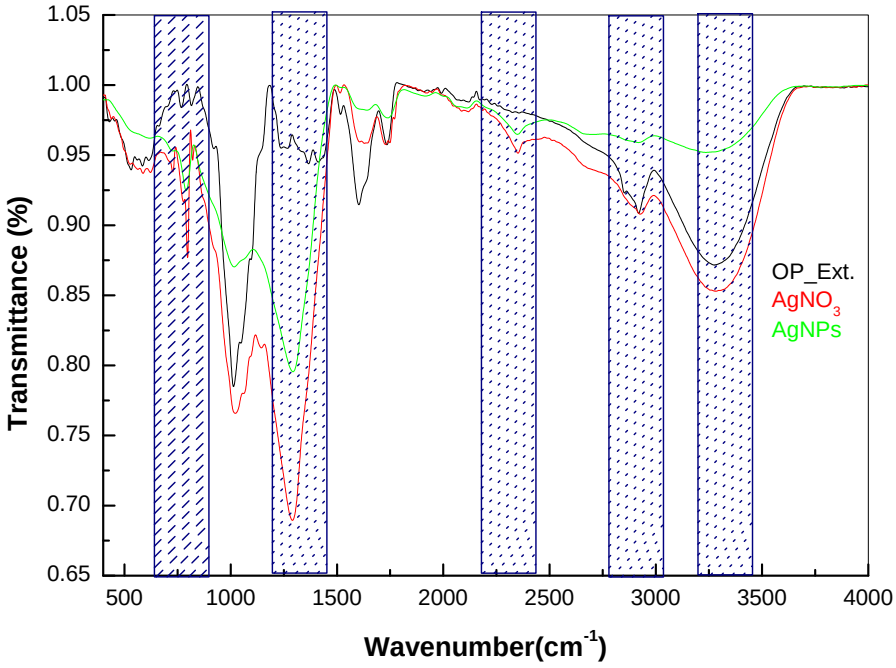

Fig. 3 FTIR spectrum of the orange peel extracts, precursor, and silver nanoparticles

3.1.4 FTIR characterization of PAN and PAN/Ag nanofibers

The FTIR spectra of PAN and PAN/AgNPs represented by Figure 4, showed a medium absorption peak at 2294 cm^{-1} assigned to C-H stretch in C-H and CH_2 groups of PAN. The band at 1447 cm^{-1} (δ_{C-H} in CH_2) represents aliphatic C-H group along PAN structure [54]. Medium band at 1356 cm^{-1} signifies O-H of the phenols from the mediated and embedded nanoparticles, respectively. The stretch at 1250 cm^{-1} was assigned to C-N bond as a result of aromatic amine. Comparing PAN and nanocomposites, it shows that the weak band with the peak was substituted by a corresponding slightly strong band. The peak at 2241 cm^{-1} was attributed to C-N stretch of acrylonitrile monomer in the polymer [55], and the transmittance shift confirmed moderate chemical interactions between the nanofibers' surface and silver nanoparticles [56].

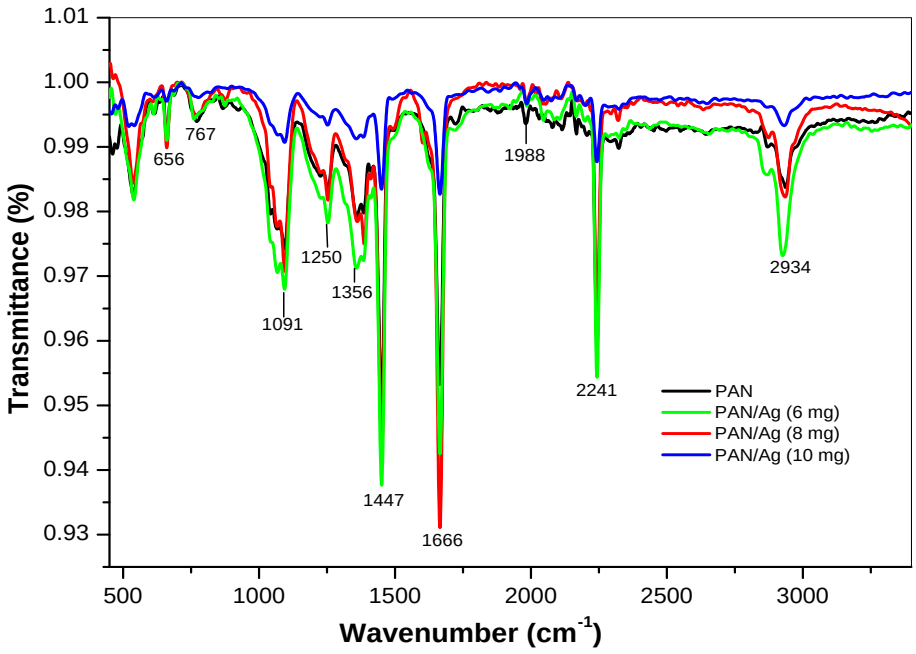

Fig. 4 FTIR spectrum of the PAN and PAN/Ag nanofibers.

3.1.5 Morphology characterization of AgNPs, PAN and PAN/Ag nanofibers (SEM)

The morphology of the synthesized nanomaterials was depicted by their respective SEM images. Figure 5 shows the SEM images of (a) Ag nanoparticles, (b) PAN, (c) PAN + 6 mg of AgNPs, (d) PAN + 8 g of AgNPs, and (e) PAN + 10 g of AgNPs. Figure 5(a) showed that the AgNPs were of spherical shape. The average diameter of AgNPs was about 20 nm and some were unevenly distributed and in aggregated form.

SEM images for PAN and Ag/PAN (Figure 5b-d) showed that nanofibers are moderately uniform in diameter, and exhibited no beads. Consequently, nanocomposites showed a decrease in average diameter as compared to pure PAN nanofibers due to gradual increasing quantity of high conductive transduction material, thus primarily confirming good electrochemical interaction with the polymer. Generally, nanofibers showed random assembly on aluminium collector plate.

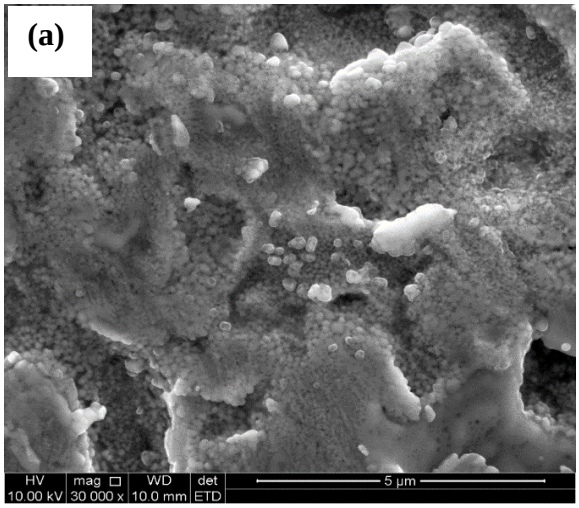
(a)
HV
10.00 kV
mag
30 000 x
WD
10.0 mm
det
ETD
5 µm

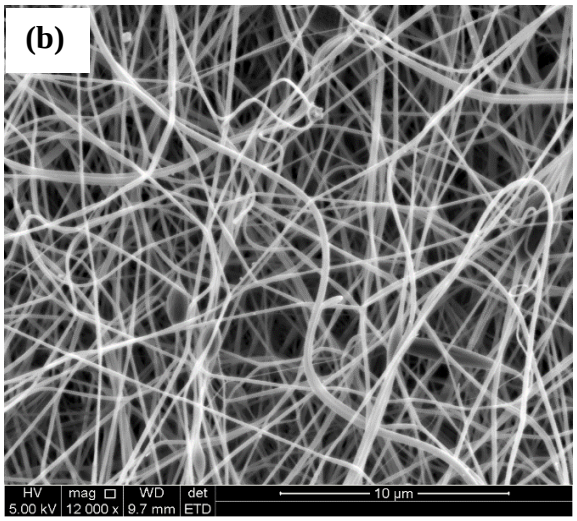
(b)
HV
5.00 kV
mag
12 000 x
WD
9.7 mm
det
ETD
10 µm

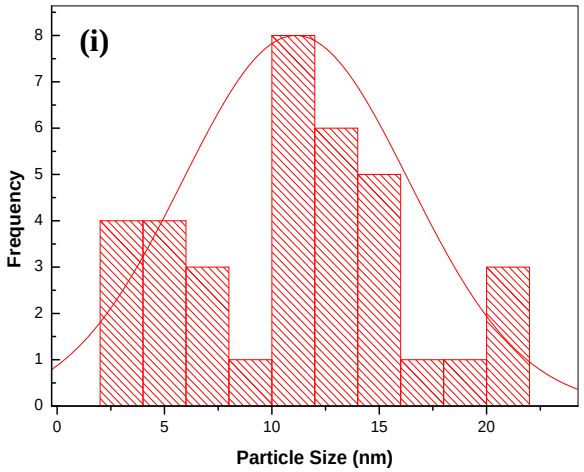
(i)
Frequency
Particle Size (nm)
0
1
2
3
4
5
6
7
8
0
5
10
15
20

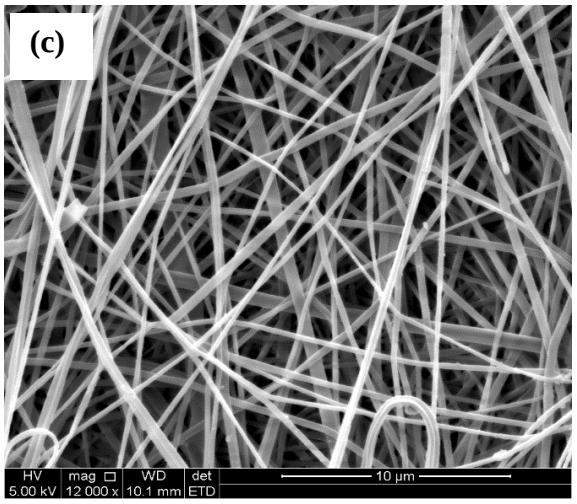
(c)
HV
5.00 kV
mag
12 000 x
WD
10.1 mm
det
ETD
10 µm

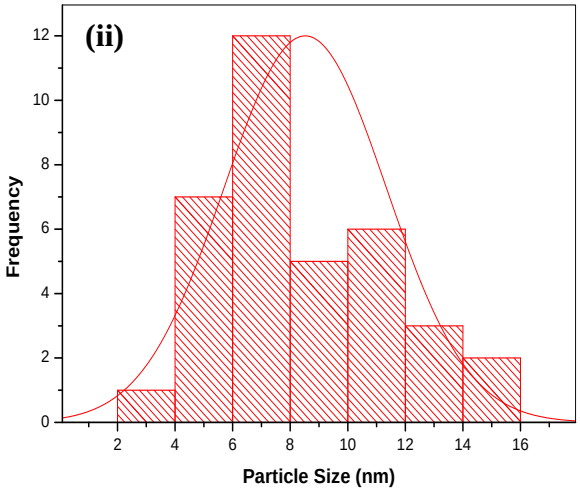
(ii)
Frequency
Particle Size (nm)
0
2
4
6
8
10
12
2
4
6
8
10
12
14
16

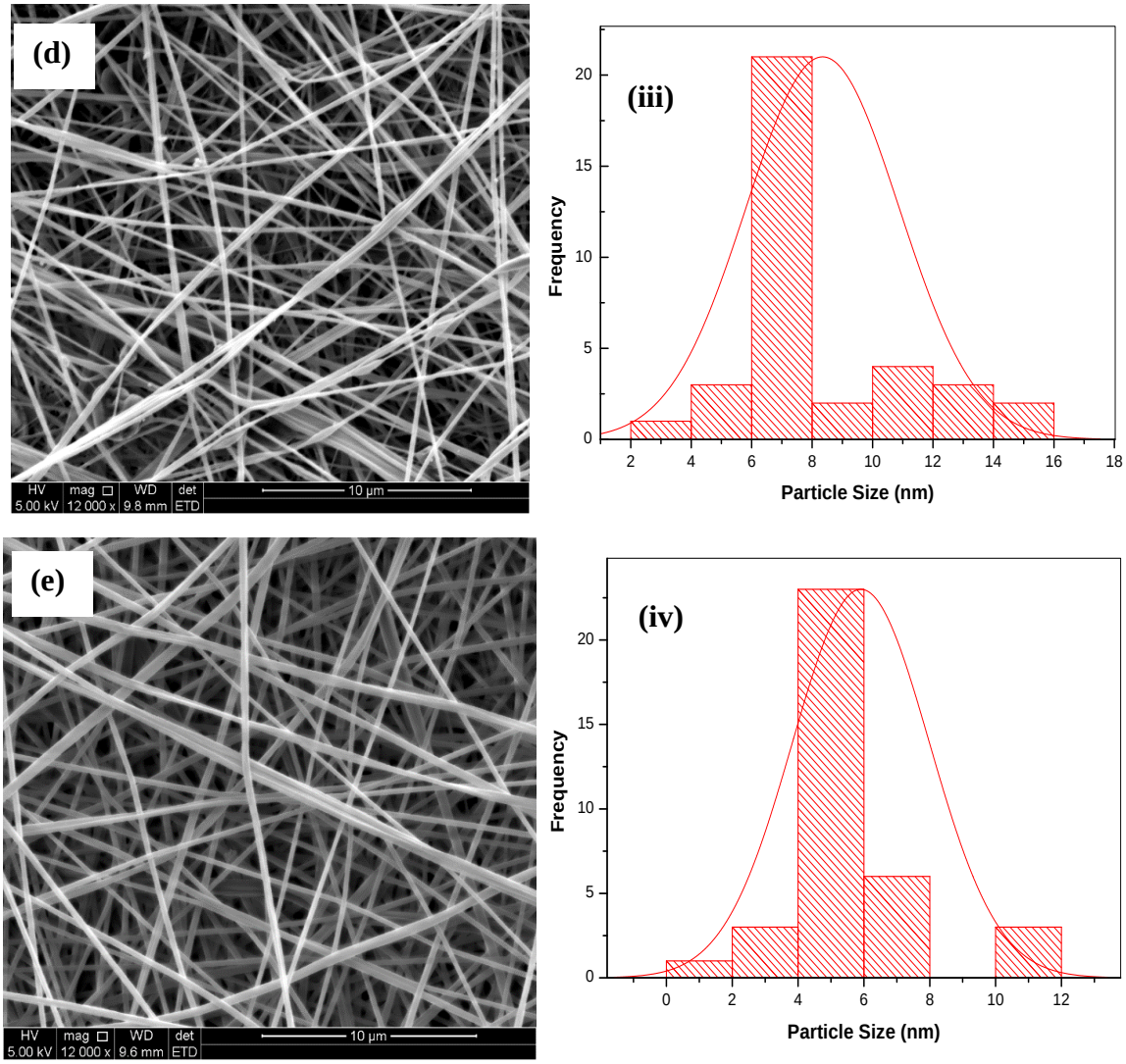

Fig. 5 SEM images of (a) AgNPs, electrospun (b) PAN (11 wt %) (c) 6mg Ag + PAN (d) 8mg Ag + PAN and (e) 10mg Ag + PAN nanofibers and diameter distributions of (i) PAN (11 wt %) (ii) 6mg Ag + PAN (iii) 8mg Ag + PAN and (iv) 10mg Ag + PAN nanofibers.

3.2 EDX study of AgNPs, PAN and PAN/Ag nanofibers

EDX spectra Fig. 6 gives insights to the elemental compositions of the nanofibers formed before and after reacting with silver nanoparticle. The EDX profile of PAN and PAN/Ag with different concentration of silver nanoparticles confirms the presence of carbon, nitrogen, and silver in the nanofiber, with oxygen which can be attributed to presence of ambient air interference with the spinning process. Furthermore, the principal element in PAN nanofiber was carbon (C = 72.46 %) and followed by nitrogen (23.04 %). Predominance of these two elements has been observed in nanocomposites too. The functionalization led to moderate inhibition of oxidation, respectively. It can be seen that the above elements and silver in the plot constitutes successful synthesis of PAN nanofibers and PAN/Ag nanocomposites (with Ag, 6 mg = 0.36 %; 8 mg= 0.62 %; 10 mg = 2.23 %).

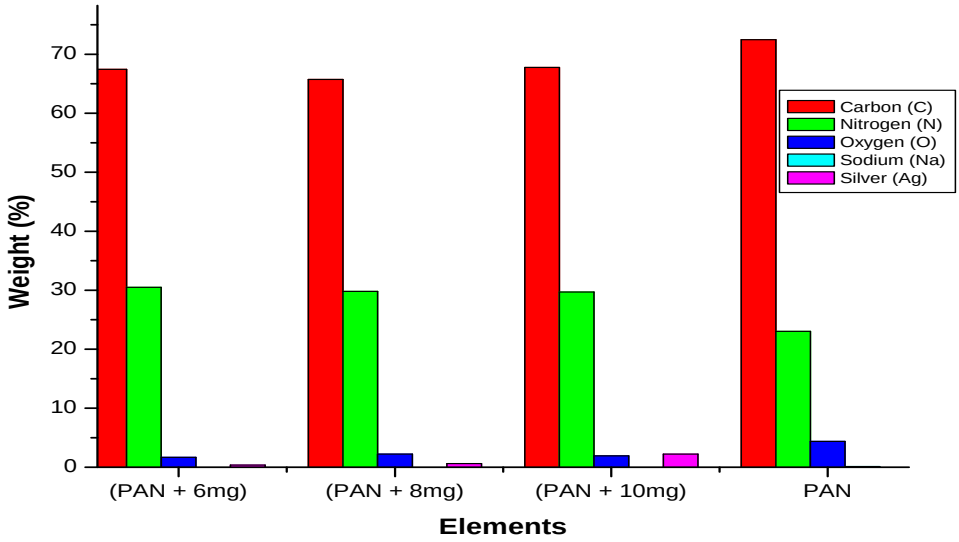

Fig. 6 EDX plot of PAN (11 wt %) and PAN/Ag nanocomposites

3.3 Zeta Potential Analysis of AgNPs

The determination of colloidal silver nanoparticles' stability was achieved through Zeta potential measurement. The obtained potential was -22.2 mV, which confirmed that the nanoparticles were moderately stable [57], and the observed deviation were 5.98. The negative potential can be as a result of capped particles with citrate ions from the reducing agent (orange peel extracts). Moreover, the potential served as evidence that the formed nanoparticle were not completely agglomerated by van de Waals attraction force as this can be seen in SEM image. Multiple potentials of dispersed silver nanoparticles have been recorded, ranging from unstable, fairly stable, and highly stable. These are -10.2 mV, − 18 mV, − 29.4 [58-60].

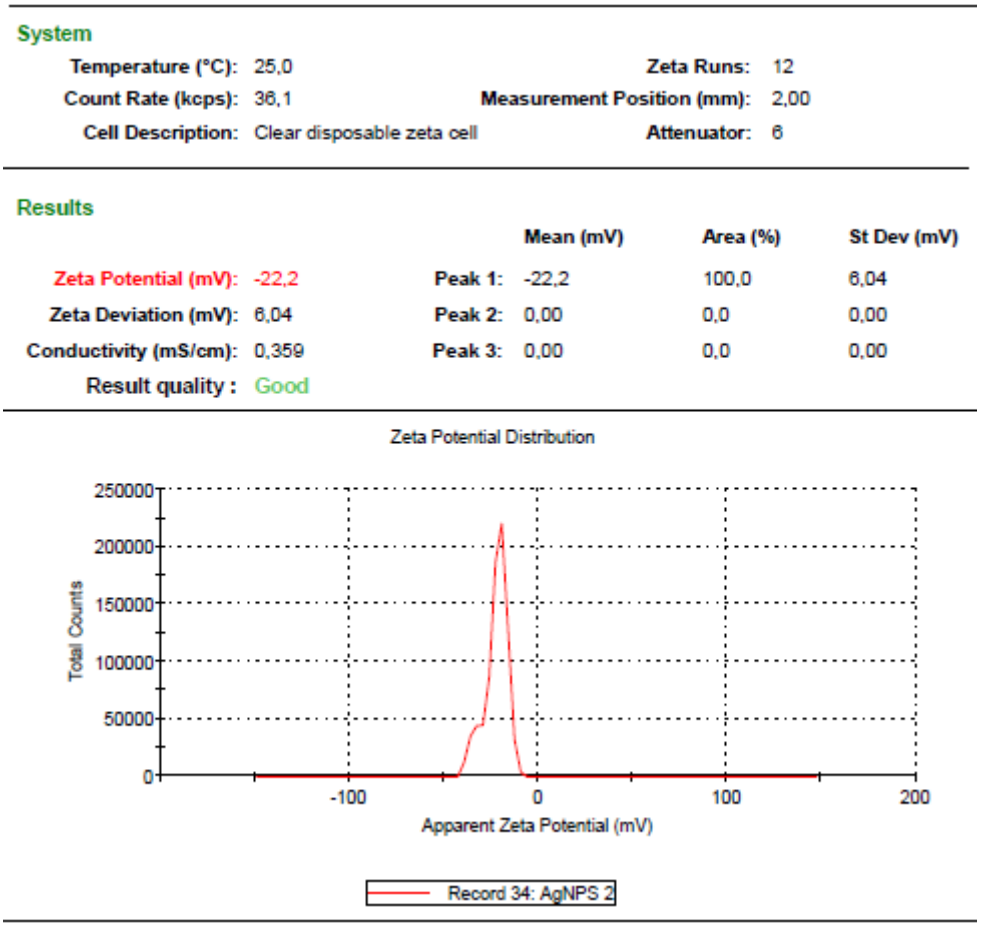

Fig. 7 Zeta potential of synthesized silver nanoparticles.

3. Conclusion

The green mediated and low cost biological silver nanoparticles and its nanocompostes were fabricated. Confirmation of particle synthesis, stability, and metal-fiber interactions were revealed by UV-Vis spectroscopy, FTIR analysis, and Zeta measurement. The surface plasmon resonance band was obtained to be 350 nm, 420 nm, and < 450 nm for PAN, PAN/Ag nanofibers and Ag nanoparticles. Evidently, as the reaction time increases, precursor and reducing agent concentration during particles fabrication depicted a proportional increase with nanoparticles' absorbance. Incorporation of nanoparticles in polyacrylonitrile polymer led to the effect on the band gap energy. The -22.2 mV Zeta potential of silver nanoparticles' colloidal suspension proved good stability and distribution, respectively. EDX study was carried out for identification of elements present in nanostructures formed. The treated silver nitrate produced fair spherical silver nanoparticles and the achieved size was 20 nm. The size of the PAN and PAN/Ag composites was evaluated as 11, 9, 8, 6 nm. Moreover, the fibers gave satisfying and decreased diameter sizes due to gradual deposition of various quantities of silver nanoparticles on polymer surface. Consequently, this functionalized polymer surface can be applied in electrical energy processes, water treatment, and catalysis studies in future.

Author Contributions

OEF conceptualized and designed the work and was part of the manuscript write-up. MGM carried out the experiments, interpreted some of the results and was also involved in the manuscript preparation. All the authors reviewed the manuscript and have agreed to its publication.

Competing financial interests: The authors declare no competing financial interests or any other conflict of interest.

Acknowledgement

OEF and MGM thank the North-West University, FRC of the Faculty of natural and Agricultural Sciences, and MaSIM for their financial support and research facilities.

References

1. Nasrollahzadeh M, Atarod M, Sajadi SM. Green synthesis of the Cu/Fe3O4 nanoparticles using Morinda morindoides leaf aqueous extract: a highly efficient magnetically separable catalyst for the reduction of organic dyes in aqueous medium at room temperature. ***Appl Surf Sci.*** 2016, 364(2016): 636-644
2. Yang X, Li Q, Wang H, Huang J, Lin L, Wang W, Wang Y, Opiyo JB, Su Y, Qingbiao L, Hong L. Green synthesis of palladium nanoparticles using broth of Cinnamomum camphora leaf. ***J Nanopart. Res.*** 2010, 12(5): 1589-1598
3. Thirumurugan A, Aswitha P, Kiruthika C, Nagarajan S, Christy AN. Green synthesis of platinum nanoparticles using Azadirachta indica–An eco-friendly approach. ***Mater Lett.*** 2016, 170(2016): 175-178
4. Aromal SA, Philip D. Green synthesis of gold nanoparticles using Trigonella foenum-graecum and its size-dependent catalytic activity. ***Spectrochim Acta A***. 2012, 97(2012): 1-5
5. Kathiraven T, Sundaramanickam A, Shanmugam N, Balasubramanian T. Green synthesis of silver nanoparticles using marine algae Caulerpa racemosa and their antibacterial activity against some human pathogens. ***Appl Nanosci.*** 2015, 5(4): 499-504
6. Das VL, Thomas R, Varghese RT, Soniya EV, Mathew J, Radhakrishnan EK. Extracellular synthesis of silver nanoparticles by the Bacillus strain CS 11 isolated from industrialized area. ***3 Biotech.*** 2014, 4(2): 121-126
7. Iravani S. Green synthesis of metal nanoparticles using plants. ***Green Chem.***, 2011, 13(10): 2638-2650
8. Ankamwar B, Chaudhary M, Sastry M. Gold nanotriangles biologically synthesized using tamarind leaf extract and potential application in vapor sensing. ***Nano-Met Chem.*** 2005, 35(1): 19-26
9. Ahmad N, Sharma S, Alam MK, Singh VN, Shamsi SF, Mehta BR, Fatma A. Rapid synthesis of silver nanoparticles using dried medicinal plant of basil. ***Colloids Surf B.*** 2010, 81(1): 81-86
10. Bankar A, Joshi B, Kumar AR, Zinjarde S. Banana peel extract mediated novel route for the synthesis of silver nanoparticles. ***Colloids Surf A.*** 2010, 368(1-3): 58-63

11. Prasad KP, Dhawale DS, Joseph S, Anand C, Wahab MA, Mano A,Vinu A. Post-synthetic functionalization of mesoporous carbon electrodes with copper oxide nanoparticles for supercapacitor application. ***Micropor Mesopor Mater.*** 2013, 172(2013): 77-86
12. Ahmed S, Ahmad M, Swami BL, Ikram S. A review on plants extract mediated synthesis of silver nanoparticles for antimicrobial applications: a green expertise. ***J Adv Res.*** 2016, 7(1): 17-28
13. Tran QH, Le AT. Silver nanoparticles: synthesis, properties, toxicology, applications and perspectives. ***Adv Nat Sci Nanosci Nanotechnol.*** 2013, 4(3): 1-20
14. De Moura MR, Mattoso LH, Zucolotto V. Development of cellulose-based bactericidal nanocomposites containing silver nanoparticles and their use as active food packaging. ***J Food Eng.*** 2012, 109(3): 520-524
15. Kalambate PK, Dar RA, Karna SP, Srivastava AK. High performance supercapacitor based on graphene-silver nanoparticles-polypyrrole nanocomposite coated on glassy carbon electrode. ***J Power Sources.*** 2015, 276(2015): 262-270
16. Andrade PF, de Faria AF, Oliveira SR, Arruda MAZ, do Carmo Gonçalves M. Improved antibacterial activity of nanofiltration polysulfone membranes modified with silver nanoparticles. ***Water Res.*** 2015, 81(2015): 333-342
17. Abaza A, Hegazy EA, Mahmoud GA, Elsheikh B. Characterization and antitumor activity of chitosan/poly (vinyl alcohol) blend doped with gold and silver nanoparticles in treatment of prostatic cancer model. ***J Pharm Pharmacol.*** 2018, 6(2018): 659-67
18. Chang G, Luo Y, Lu W, Qin X, Asiri AM, Al-Youbi AO, Sun X. Ag nanoparticles decorated polyaniline nanofibers: synthesis, characterization, and applications toward catalytic reduction of 4-nitrophenol and electrochemical detection of H_2O_2 and glucose. ***Catal Sci Tech.*** 2012, 2(4): 800-806
19. Choudhury A. Polyaniline/silver nanocomposites: Dielectric properties and ethanol vapour sensitivity. ***Sens Actuators B Chem.*** 2009, 138(1): 318-325
20. Tu D, Pagliara S, Camposeo A, Persano L, Cingolani R, Pisignano D. Single light-emitting polymer nanofiber field-effect transistors. ***Nanoscale.*** 2010, 2(10): 2217-2222
21. Zhang Y, Kim JJ, Chen D, Tuller HL, Rutledge GC. Electrospun polyaniline fibers as highly sensitive room temperature chemiresistive sensors for ammonia and nitrogen dioxide gases. ***Adv Funct Mater.*** 2014, 24(25): 4005-4014
22. Číková E, Mičušík M, Šišková A, Procházka M, Fedorko P, Omastová M. Conducting electrospun polycaprolactone/polypyrrole fibers. ***Synth. Met.*** 2018, 235(2018): 80-88
23. Song Z, Chiang SW, Chu X, Du H, Li J, Gan L, Xu C, Yao Y, He Y, Li B, Kang F. Effects of solvent on structures and properties of electrospun poly (ethylene oxide) nanofibers. ***J Appl Polym Sci.*** 2018, 135(5): 45787-45797
24. Qiao Z, Xie Y, Xu J, Zhu Y, Qian Y. Synthesis of CdS/polyacrylonitrile nanocomposites by γ-irradiation. ***Mater Res Bull.*** 2000, 35(8): 1355-1360
25. Liu H, Ge X, Ni Y, Ye Q, Zhang Z. Synthesis and characterization of polyacrylonitrile–silver nanocomposites by γ-irradiation. ***Radiat Phys Chem.*** 2001, 61(1): 89-91
26. Qiao Z, Xie YI, Zhu Y, Qian Y. Synthesis of PbS/polyacrylonitrile nanocomposites at room temperature by γ-irradiation. ***J Mater Chem.*** 1999, 9(4): 1001-1002
27. D. G. Muratov, E. V.Yakushko, L. V. Kozhitov, A. V. Popkova and M. A. Pushkarev, ***Modern Electro Mater.*** 2016, 2: 70-73
28. Choi YS, Wang KH, Xu M, Chung IJ. Synthesis of exfoliated polyacrylonitrile/Na− MMT nanocomposites via emulsion polymerization. ***Chem Mater.*** 2002, 14(7): 2936-2939

29. Kizildag N, Ucar N, Onen A. Nanocomposite polyacrylonitrile filaments with titanium dioxide and silver nanoparticles for multifunctionality. ***J Ind Text.*** 2018, 47(7), 1716-1738
30. Zhang D, Chung R, Karki AB, Li F, Young DP, Guo Z. Magnetic and magnetoresistance behaviors of solvent extracted particulate iron/polyacrylonitrile nanocomposites. ***J Phys Chem C.*** 2009, 114(1): 212-219
31. Selvam AK, Nallathambi G. Polyacrylonitrile/silver nanoparticle electrospun nanocomposite matrix for bacterial filtration. ***Fiber Polym.*** 2015, 16(6): 1327-1335
32. Mohsenibandpey A, Eslami A, Maleh HK, Rabori MM. Investigating the efficiency of nanocomposite membranes synthesized by polyacrylonitrile polymers containing single-walled carbon nanotubes in decreasing chemical and biological pollution indicators of greywater. ***Bulg Chem Commun.*** 2016, 48(2016): 102-111
33. Luo Q, Yang X, Zhao X, Wang D, Yin R, Li X, An J. Facile preparation of well-dispersed ZnO/cyclized polyacrylonitrile nanocomposites with highly enhanced visible-light photocatalytic activity. ***Appl Catal B.*** 2017, 204(2017): 304-315
34. Li X, Peng T, Zhang Y, Wen Y, Nan Z. A new efficient visible-light photocatalyst made of SnO_2 and cyclized polyacrylonitrile. ***Mater Res Bull.*** 2018, 97(2018), 517-522
35. Shojaei M, Sadjadi S, Rajabi-Hamane M, Ahmadi SJ. Synthesis of TiO2/polyacrylonitrile nanofibers composite and its application to lead ions removal from waste waters. ***Desalination Water Treat.*** 2015, 56(5): 1403-1412
36. Yao LR, Song XM, Zhang GY, Xu SQ, Jiang YQ, Cheng DH, Lu YH. Preparation of Ag/HBP/PAN nanofiber web and its antimicrobial and filtration property. ***J Nanomater.*** 2016, 2016(2016): 86-96
37. Kharaghani D, Khan M, Shahzad A, Inoue Y, Yamamoto T, Rozet S, Tamada Y, Kim I. . Preparation and in-vitro assessment of hierarchal organized antibacterial breath mask based on polyacrylonitrile/silver (PAN/AgNPs) nanofiber. ***Nanomater.*** 2018, *8*(7): 461-472
38. Thakur M, Sinsabaugh SL, Isaacson MJ, Wong MS, Biswal SL. Inexpensive method for producing macroporous silicon particulates (MPSPs) with pyrolyzed polyacrylonitrile for lithium ion batteries. ***Sci Rep.*** 2(2012): 795
39. Parekh S, David R, Bannuru K, Krishnaswamy L, Baji A. Electrospun silver coated polyacrylonitrile membranes for water filtration applications. ***Membranes.*** 2018, 8(3): 59-69
40. Lala NL, Ramaseshan R, Bojun L, Sundarrajan S, Barhate RS, Ying-jun L, Ramakrishna S. Fabrication of nanofibers with antimicrobial functionality used as filters: protection against bacterial contaminants. ***Biotechnol Bioeng.*** 2007, 97(6): 1357-1365
41. Pandey N, Shukla SK, Singh NB. Water purification by polymer nanocomposites: An overview. ***Nanocomposites.*** 2017, 3(2): 47-66
42. Zhang S, Tang Y, Vlahovic B. A review on preparation and applications of silver-containing nanofibers. ***Nanoscale Res Lett.*** 2016, 11(1): 80-88
43. Liu Y, Jiang G, Li L, Chen H, Huang Q, Jiang T, Du X. Silver nanoparticles supported on electrospun polyacrylonitrile nanofibrous mats for catalytic applications. ***MRS Commun.*** 2016, 6(1): 31-40
44. Hyllested JÆ, Palanco ME, Hagen N, Mogensen KB, Kneipp K. Green preparation and spectroscopic characterization of plasmonic silver nanoparticles using fruits as reducing agents. ***Beilstein J Nanotechnol.*** 2015, 6: 293-299

45. Halawani EM. Rapid biosynthesis method and characterization of silver nanoparticles using Zizyphus spina christi leaf extract and their antibacterial efficacy in therapeutic application. ***J Biomater Nanobiotechnol.*** 2016, 8(1): 22-35
46. Carrillo-López LM, Zavaleta-Mancera HA, Vilchis-Nestor A, Soto-Hernández RM, Arenas-Alatorre J, Trejo-Téllez LI, Gómez-Merino F. Biosynthesis of silver nanoparticles using Chenopodium ambrosioides. ***J Nanomater.*** 2014, 2014(198): 198-206
47. Ahmed S, Ahmad M, Swami BL, Ikram S. Green synthesis of silver nanoparticles using Azadirachta indica aqueous leaf extract. ***J Radiat Res Appl Sci.*** 2016, *9*(1): 1-7
48. Jain N, Bhargava A, Majumdar S, Tarafdar JC, Panwar J. Extracellular biosynthesis and characterization of silver nanoparticles using Aspergillus flavus NJP08: A mechanism perspective. ***Nanoscale Res Lett.*** 2011, 3(2): 635-641
49. Zhang XF, Liu ZG, Shen W, Gurunathan S. Silver nanoparticles: Synthesis, characterization, properties, applications, and therapeutic approaches. ***Int J Mol Sci.*** 2016, 17(9): 1534-1567
50. Kalimuthu K, Babu RS, Venkataraman D, Bilal M, Gurunathan S. Biosynthesis of silver nanocrystals by Bacillus licheniformis. ***Colloids Surf B.*** 2008, 65(1): 150-153
51. Gharibshahi L, Saion E, Gharibshahi E, Shaari AH, Matori KA. Structural and optical properties of Ag nanoparticles synthesized by thermal treatment method. ***Mater.*** 2017, 10(4): 402-414
52. Prathna TC, Chandrasekaran N, Raichur AM, Mukherjee A. Biomimetic synthesis of silver nanoparticles by Citrus limon (lemon) aqueous extract and theoretical prediction of particle size. ***Colloids Surf B.*** 2011, 82(1): 152-159
53. Saquing CD, Manasco JL, Khan SA. Electrospun nanoparticle–nanofiber composites via a one-step synthesis. ***Small.*** 2009, 5(8): 944-951
54. Ouyang Q, Cheng L, Wang H, Li K. Mechanism and kinetics of the stabilization reactions of itaconic acid-modified polyacrylonitrile. ***Polym Degrad Stab.*** 2008, 93(8): 1415-1421
55. Ribeiro RF, Pardini LC, Alves NP, Júnior B, Rios CA. Thermal Stabilization study of polyacrylonitrile fiber obtained by extrusion. ***Polimeros.*** 2015, 25(6), 523-530
56. Dong F, Li Z, Huang H, Yang F, Zheng W, Wang C. Fabrication of semiconductor nanostructures on the outer surfaces of polyacrylonitrile nanofibers by in-situ electrospinning. ***Mater Lett.*** 2007, 61(11-12): 2556-2559
57. Bhattacharjee S. DLS and zeta potential–What they are and what they are not? ***J Control Release.*** 2016, 235 (2016): 337-351
58. Patra S, Mukherjee S, Barui A K, Ganguly A, Sreedhar B, Patra CR. Green synthesis, characterization of gold and silver nanoparticles and their potential application for cancer therapeutics. ***Mater Sci Eng C.*** 2015, 53 (2015): 298-309
59. Mittal AK, Tripathy D, Choudhary A, Aili PK, Chatterjee A, Singh IP, Banerjee UC. Bio-synthesis of silver nanoparticles using Potentilla fulgens Wall. ex Hook. and its therapeutic evaluation as anticancer and antimicrobial agent. ***Mater Sci Eng C.*** 2015, 53 (2015): 120-127
60. Nayak D, Ashe S, Rauta PR, Kumari M, Nayak B. Bark extract mediated green synthesis of silver nanoparticles: Evaluation of antimicrobial activity and antiproliferative response against osteosarcoma. ***Mater Sci Eng C***. 2016, 58 (2016): 44-52